Colloid Polym Sci (2009) 287:1237–1242
DOI 10.1007/s00396-009-2092-2

SHORT COMMUNICATION

Effect of temperature gradient on the development of β phase polypropylene in dynamically vulcanized PP/EPDM blends

Xue-Gang Tang · Wei Yang · Gui-Fang Shan · Bin Yang · Bang-Hu Xie · Ming-Bo Yang · Meng Hou

Received: 28 April 2009 / Revised: 30 July 2009 / Accepted: 3 August 2009 / Published online: 25 August 2009

Abstract Different sample thicknesses were adopted to investigate the effect of temperature gradient on the development of β phase polypropylene (PP) in the compression-molded dynamically vulcanized thermoplastic elastomers (TPVs) based on PP/ethylene-propylene-diene rubber blend. Differential scanning calorimetry and wide-angle X-ray diffraction were employed to study the melting behavior and crystalline structures. The results indicated that the content of β phase increased with the sample thickness of TPV increasing, while the total crystallinity of PP almost kept constant. The simulation of the temperature field showed that there was a temperature gradient along the direction of sample thickness, and the strength of the temperature gradient increased with the thickness of TPV increasing. The reason for the change of β phase content was found to lie in the reduction of the entropy in the temperature gradient field, which was a result from the decrease of the molecular chain conformation.

Keywords Temperature gradient field · β phase · Dynamically vulcanized PP/EPDM blend (TPV)

X.-G. Tang · M. Hou (✉)
Division of Mechanical Engineering, School of Engineering,
The University of Queensland,
Queensland 4072, Australia
e-mail: m.hou@uq.edu.au

W. Yang (✉) · G.-F. Shan · B. Yang · B.-H. Xie · M.-B. Yang
College of Polymer Science and Engineering, Sichuan University,
State Key Laboratory of Polymer Materials Engineering,
Chengdu 610065 Sichuan, China
e-mail: ysjsanjin@163.com

Introduction

It is well-known that the temperature field has a profound effect on the formation of polymer crystals, which may affect the rate of crystallization and the thickness of crystal lamella, and the situation is more distinct for polypropylene (PP). Isotactic polypropylene (iPP) is a polymorphic material, having at least four modifications of crystals: monoclinic (α), hexagonal (β), triclinic (γ), and smectic [1–6]. Different temperature fields will result in different crystal modifications. Using some special techniques can obtain polypropylene rich in β modifications, such as the crystallization at high undercooling [7, 8] and the crystallization in a temperature gradient field [9, 10].

The temperature dependencies of both the spherulite nucleation and growth rate result in significant differences in the crystallization kinetics and in the final spherulite structure between regions solidifying at different temperatures. It is also known that the temperature gradient leads to anisotropic spherulite growth and shapes and affects the directions of spherulite growth. The growth trajectories bend in the temperature gradient, being normal to the growth front [11–13]. The changes in interspherulitic boundary shapes have also been reported [11, 13]. Recently, Pawlak and Piorkowska [13] reported that the temperature gradient could accelerate the conversion of the melt into spherulites. At the same time, Choi et al. [14] have investigated the effect of temperature gradient on polymer dynamics due to an imposed flow field. The diffusion equation and concentration profile of the polymer molecules induced by a temperature gradient using a two-bead dumbbell model have been obtained from the Fokker–Planck equation. From the concentration equation constructed for a dilute solution in general flow geometry, they find that there are significant effects on the polymer migration not only due

to the nonhomogeneity of the flow field, but also due to the temperature gradients.

The β modification of iPP (β-iPP) has several advantageous properties, especially high impact strength compared with α form PP [15–17]. To improve the impact toughness of PP, especially iPP, various elastomers have been introduced, such as ethylene-propylene rubber, styrene-butadiene-styrene copolymer, butyl rubber, and ethylene-propylene-diene rubber (EPDM) [18–25]. Among these rubbers, EPDM is considered to be one of the most effective impact modifiers for PP. Further improvement in performances of PP/EPDM blends can be gained by dynamic vulcanization [26–29]. Thermoplastic vulcanizates or TPVs are blends where the elastomeric component is vulcanized in situ during melt mixing with the thermoplastic component at high shear and elevated temperature. The resulting blend has small, uniform, and finely distributed cross-linked rubber particle in the matrix. It has been shown that dynamic cross-linking of EPDM during its melt mixing with iPP can improve some properties of the blend and even results in high impact PP-based materials.

In our previous studies on the dynamically vulcanized PP/EPDM blends, we found that the presence of β crystals of PP induced by nucleating agents could greatly improve the fracture toughness of the blend, and the development of β phase PP was related to the morphology confining effect [30, 31]. In this work, we focus on the effect of temperature field on the development of β phase PP in dynamically vulcanized PP/EPDM blends, which will help us clearly describe the development of β phase PP in such a multiphase system and provide valuable guidance in the design and preparation of high performance PP blends.

Experimental procedure

Material

The β nucleating agent (β-NA) used in this study was WBG-II, a powder composed of rare-earth organic compounds and purchased from Guangdong Weilinna Functional Material Company Ltd. iPP, with the trademark F401 which was obtained from Lanzhou Petrochemical Company Ltd. Certain properties of the resin, provided by manufacturer, are MFR=2.5 g/10 min according to ASTM D1238.79, density=0.91 g·cm^{-3} according to ASTM D1505-68, and a tacticity of 98%. EPDM (Nordel 4725p) was obtained from Dupont Dow Elastomers L.L.C., Wilmington, DE, USA. It contains 70% ethylene and 4.9% ethylidene norbornene with a Mooney viscosity ($ML_{2+10}^{125^\circ C}$) and $\overline{M}_w$ of 25 and 135,000 g·mol^{-1}, respectively. Phenolic resin (PF) was obtained from Yuan Tai Biochemistry Industry Company Ltd. with the trademark TXL-201. Its softening point is 75 to 95 °C; the content of methylol, 6.0–7.5%; the content of water, ≤1.0%; and the content of bromine, ≤4.0%.

Sample preparation

The melt reactive blending process for preparing TPV samples (PP:EDPM=5:5 wt) was carried out in an SHJ-20 corotating twin–screw extruder with a screw diameter of 25 mm, a length/diameter ratio of 23, and a temperature profile of 170, 180, 190, and 185 °C from the feeding zone to the die. The content of β-NA was 0.3 wt% (to the weight of the blends). The PF content is 6 wt% (to the weight of the blends). Polypropylene, EPDM, PF, and β-NA were simply mixed first, and then added to the twin–screw extruder. The extrudate was then pelletized. The pellets were dried, and injection was molded into dumbbell tensile samples and rectangular impact samples on a PS40E5ASE precise injection-molding machine with a temperature profile of 170, 190, 200, and 195 °C from the feeding zone to the nozzle. Both the injection pressure and the holding pressure were 37.4 MPa. The obtained samples were heat pressed for 10 min on a compression molding machine ($XLB-D400\times400\times2$) into 1 mm thick sheet, with a temperature of 200 °C, and a pressure of 10 MPa. The compression-molded sheet was then cooled to room temperature under pressure and used for test after 24 h storage at room temperature.

Samples of different thickness for tests were prepared by gently grinding the compression-molded sheet on abrasive papers. Then, these samples were heat-treated on a hot stage with a temperature accuracy of ±0.1 °C. Figure 1 shows the layout of the heat treatment of the samples. The samples were heated to 200 °C at a rate of 10 °C/min and held at 200 °C for 5 min to eliminate any thermal history, and afterward, the samples were cooled to 20 °C at a rate of 10 °C/min.

Tests

Differential scanning calorimetry

The melting behaviors of the heat-treated samples were studied by means of a TA Q20 differential scanning

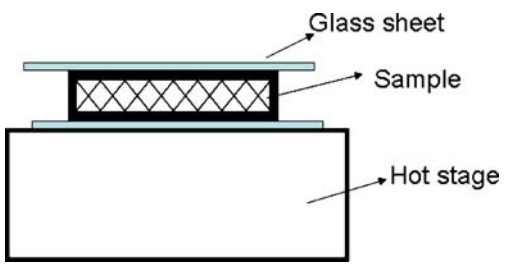

Fig. 1 The schematic presentation of the layout of the heat treatment of the samples

calorimeter. The samples, of about 5 mg, cut along the normal direction of the contact surface with the hot stage, were heated to 200 °C at a heating rate of 10 °C/min. The temperature and heat flow scales were calibrated using high-purity indium and zinc samples.

Wide-angle X-ray diffraction

Wide-angle X-ray diffraction (WAXD) measurements were carried out with a DX-1000 X-Ray diffractometer at room temperature. The Cu K-alpha (wave length=0.154056 nm) irradiation source was operated at 50 kV and 30 mA. Patterns were recorded by monitoring diffractions from 5° to 50°, and the scanning speed was 3°/min. The scanning surface is the contact surface with the hot stage. The relative content of β phase (K_β) in the samples was calculated from WAXD diffractograms according to Turner-Jones et al. [32],

$$K_\beta = \frac{H^\beta_{300}}{H^\alpha_{110} + H^\alpha_{040} + H^\alpha_{130} + H^\beta_{300}} \quad (1)$$

where H^α_{110}, H^α_{040}, and H^α_{130} are the intensity of the (110), (040), and (130) reflections of α phase appearing at 2θ around 14.1°, 16.9°, and 18.5°, respectively, and H^β_{300} is the intensity of (300) reflection of β phase at 2θ around 16.0°. Here, all the diffraction data were corrected for background (air and instrument) scattering before analysis. The diffraction patterns were analyzed using a MDI Jade 5.0 software (Materials Data Inc., Liverpool, Canada).

Results and discussion

Crystalline structures

Figure 2 shows the melting behaviors of the compression-molded TPV samples with different thicknesses. Two distinct melting peaks can be seen clearly for all the samples. The lower one being the characteristic melting peak for β phase PP and the higher one is the characteristic melting peak for α phase PP. It can also be observed that with the increase of sample thickness, the height of melting peak for β phase PP increases, and the temperature of the melting peaks increases too, both of which mean that higher content of β phase PP with higher degree of perfection was presented in TPV samples with larger thickness.

To further ensure the crystalline structures, WAXD measurements were carried out, and the results are shown in Fig. 3. The WAXD patterns of TPVs show five distinct peaks at 2θ of about 14.1°, 16.9°, 18.5°, 21.2°, and 21.9°, respectively, which correspond to the (110), (040), (130), (131), and (111) reflections of α-iPP indicating the existence of α phase. There is also a peak at about 16.0° which corresponds to the (300) reflection of β phase of iPP. At the same time, a profound change can be found at the intensity of the characteristic peak of β phase, i.e., the (300) reflection changes a lot with the sample thickness changing, which shows that the sample thickness has a distinct effect on the development of the β crystals. The intensity of the characteristic peak of β phase increases with increasing sample thickness. To know better about the changes, we use Eq. 1 to calculate K_β. For samples with different thickness, different K_β values are obtained for the blends as illustrated in Fig. 4, which shows clearly that the K_β value increases distinctly with the sample thickness increasing. Figure 5 shows the total crystallinity of the compression-molded TPVs according to WAXD measurements from which it can be found that the total crystallinity almost keeps constant with sample thickness of the TPV increasing.

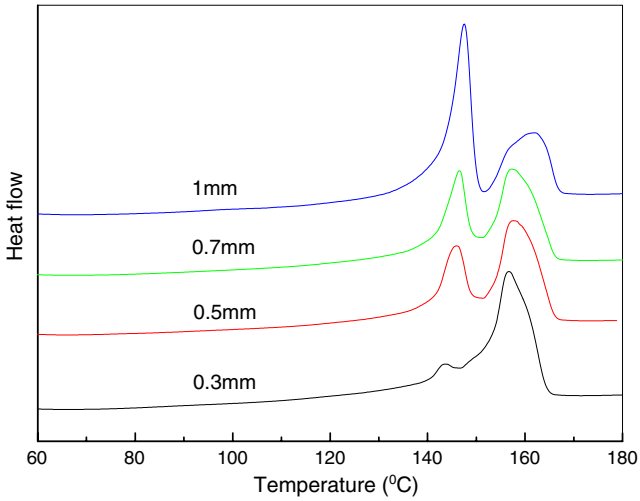

Fig. 2 The melting behaviors of the compression-molded TPVs with different thickness

The temperature field

Aiming at clarifying the influence of temperature field on the development of β phase, clearly, the one-dimensional phase change heat conduction behaviors of the sample during the cooling stage were simulated using Cao and Faghri's enthalpy transformation method. This method shows good adaptivity in solving heat conduction problems with latent heat effects, and the simulated results showed a good agreement with the experimental data in our previous work [33, 34]. Through the discretization and iterative process of the control-volume/finite-difference method, the development of the temperature as a function of the cooling time at various locations in the samples can be predicted, and the positions for temperature simulation were consistent with that in WAXD measurement. Five positions with

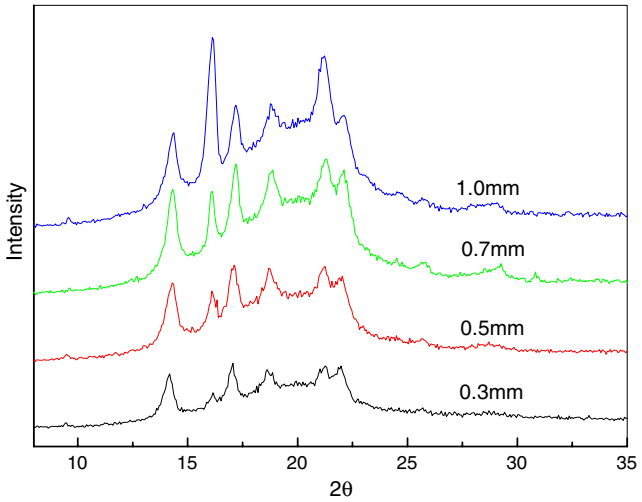

Fig. 3 WAXD patterns of compression-molded TPVs with different thickness

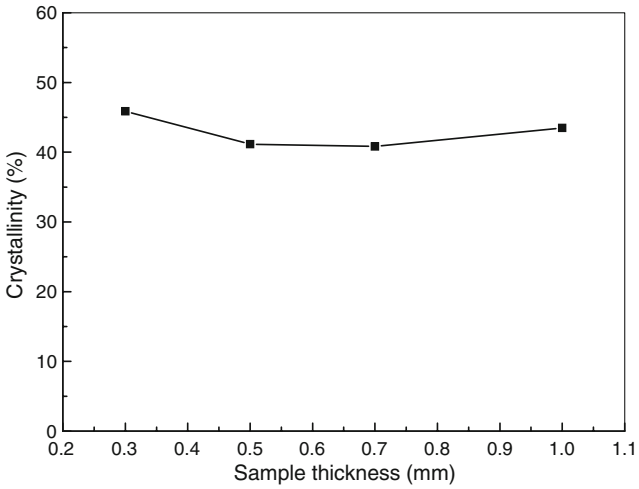

Fig. 5 Effect of sample thickness on the crystallinity of the compression-molded TPVs

the same distance across the thickness direction have been selected and marked as position a, position b, position c, position d, and position e as shown in Fig. 6.

For the calculation, the thermal conductivity K was measured using Hot Disk TPS 2500, and the specific heat (C_s, C_l), the latent heat (L), and phase change temperature range (T_1~T_2) were obtained through modulated DSC at DSC Q100 V9.5 Build 288. In addition, the density of TPV/β-NA was taken as the weight average of the density of PP and EPDM, which were provided by the manufacturers. The related parameters of the TPV samples are listed in Table 1.

Figure 7 shows the temperature distribution during the cooling of the sample with a thickness of 1 mm. It can be seen clearly that for the TPV sample, the temperature variation of each layer is not the same, which results in a temperature gradient along the direction of sample thickness in the course of cooling in the compression mold. The same phenomenon is also found in the other samples, but the strength of the temperature gradient for samples of different thickness is not the same (to simplify the expression in this research, the strength of temperature gradient was defined as the temperature difference divided by the thickness). From Fig. 8, it can be seen that the strength of temperature gradient increases with the increasing of sample thickness. The thicker the sample, the more time needed to dissipate the heat and the stronger the temperature gradient occurred.

Discussion

The processes of crystallization and crystal growth, like many other processes in chemistry, are controlled by thermodynamic and kinetic factors. Thermodynamics will dictate the preferred lowest energy state, but the rate at which this state is achieved depends on the processes involved in the molecular attachment—kinetic factors [35]. The classical approach to crystal growth considers the thermodynamic changes that occur in crystallization [36].

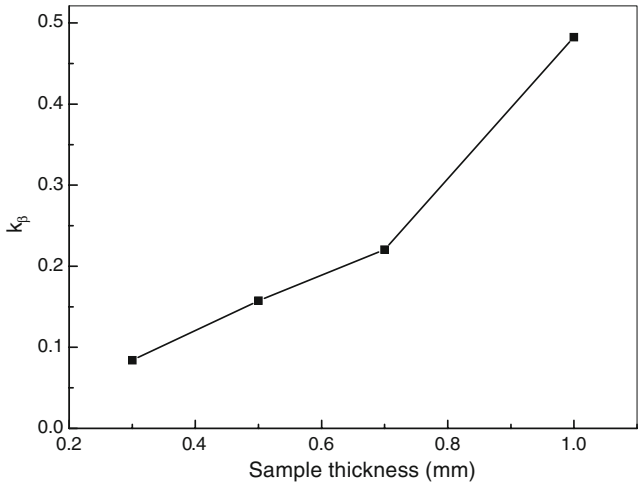

Fig. 4 Effect of sample thickness on the K_β value of the compression-molded TPVs

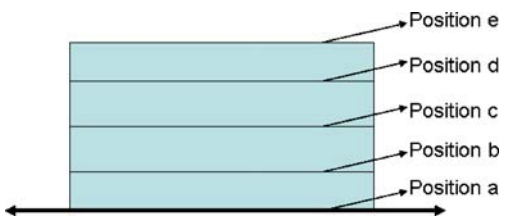

Fig. 6 The schematic presentation of the simulated positions in the TPV samples

Table 1 Related parameters of TPV/β-NA

p (kg m^{-3})	K (W•m^{-1}°C^{-1})	C_s (J•kg^{-1}°C^{-1})	C_l (J•kg^{-1}°C^{-1})	L (J•kg^{-1})	T_1~T_2(°C)
889.9	0.2395	2287.2	2627.2	37750.0	122.3~135.0

The overall free energy difference, ΔG, can be expressed as:

$$\Delta G = \Delta H - T\Delta S \quad (2)$$

There are a lot of researches concerned with the temperature gradient field. Lee et al. studied the polymerization-induced phase separation (spinodal decomposition) in a model binary polymer solution under a linear spatial temperature gradient for the purpose of fabricating anisotropic polymeric materials by using mathematical modeling and computer simulation. Their results showed that an anisotropic morphology could be obtained when a temperature gradient field was imposed along the polymer solution sample [37]. Li et al. performed small-angle Rayleigh light-scattering measurements in polymer solutions under various externally applied temperature gradients and confirmed the existence of an enhancement of the concentration fluctuations [38]. Choi et al. investigated the effect of temperature gradient on polymer dynamics due to an imposed flow field and found that there were significant effects on the polymer migration, not only due to the nonhomogeneity of the flow field, but also due to temperature gradients [14].

In a temperature gradient field, the molecules usually move along the temperature gradient. Many investigations dealt with the thermophoresis of small particles suspended in a gas in which a temperature gradient existed. The particles experience a force in the direction opposite to that of the temperature gradient and, thereby, move toward the cooler region [39, 40]. In fluid mixtures, the temperature gradient induces a concentration gradient through the Soret effect [41]. At the same time, some other studies show that temperature gradient leads to anisotropic spherulite growth and shapes and affects the directions of spherulite growth. The growth trajectories bend in the temperature gradient, being normal to the growth front [11–13]. So, it can be seen that the molecules do move along the temperature gradient.

For macromolecules, which are long-chain molecules, we think that they will orient along the temperature gradient because the molecules in high temperature have larger mobility than those in low temperature. It is well-known that $S=k\ln W$, in which W is the probable configuration. With the orientation of the macromolecules, the probable configuration will decrease leading to the reduction of the entropy.

Just according to Eq. 2, it can obtain the conclusion directly that the reduction of entropy can lead the increase of the free energy. Generally, iPP crystallizes into the α phase (α-iPP) under processing conditions used in the industrial practice because compared with β phase, α phase has lower energy, so the energy barrier for the formation of α phase is lower. However, in the temperature gradient field, the situations are different because of the reduction of the entropy or the increase in the ΔG, which will be higher than the energy level in the system to overcome the energy barrier and finally form crystal with higher energy level. In the TPVs studied in this work, for the TPV sample with the thickness of 1 mm, a large reduction of the ΔS occurs because of the strong temperature gradient field. So, it is

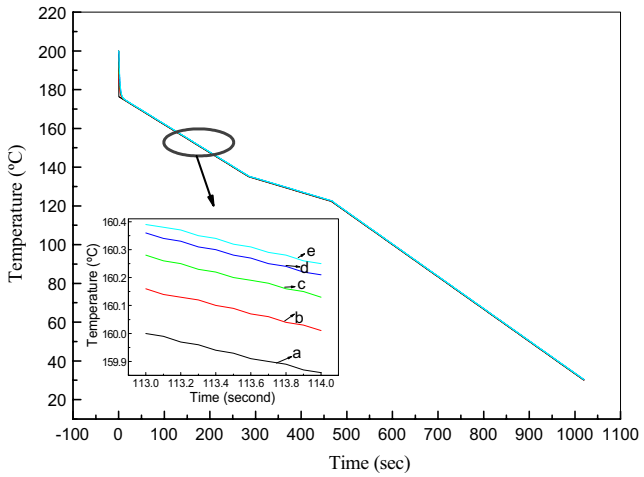

Fig. 7 Simulated cooling temperature profiles at various locations for the TPV sample with the thickness of 1 mm

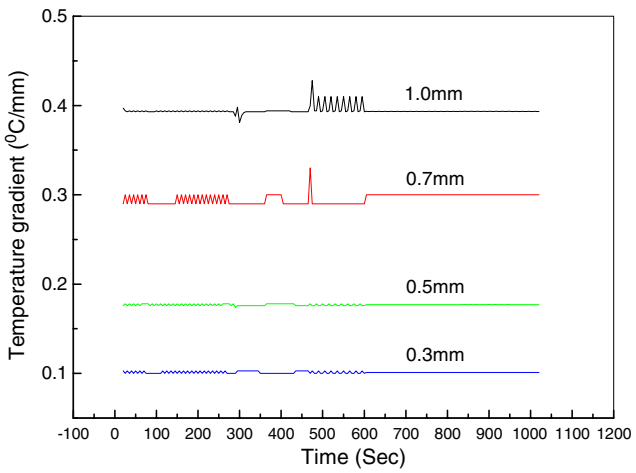

Fig. 8 The strength of the temperature gradient of samples with different thickness

easier to overcome the energy barrier to form β phase and, finally, more β phase PP forms. However, for the TPV sample with the thickness of 0.3 mm, the temperature gradient field is so weak that the reduction of the ΔS is limited. Thus, the content of β phase PP-formed is lower.

Conclusion

The DSC and WXRD results showed that the content of β phase was affected by the sample thickness of the dynamically vulcanized TPV based on PP/EPDM blends experienced the same heat treatment procedure. It was found that with the increasing of the sample thickness, the content of β phase increased, while the total crystallinity almost kept constant. The simulation of the temperature field showed that there was a temperature gradient along the direction of sample thickness, and the strength of temperature gradient increased with the sample thickness increasing. The reason for the changing of the content of β phase may lie in the reduction of the entropy during the temperature gradient, resulting from decrease of the molecular chain conformation.

Acknowledgements The authors gratefully acknowledge the financial support of National Natural Science Foundation of China (grant number 20734005), the Program for New Century Excellent Talents in University (NCET-08-0382), Doctoral Research Foundation granted by the National Ministry of Education, China (grant number 20060610029), the Special Funds for Major Basic Research of China (grant number 2005CB623808), and the support from International Postgraduate Research Scholarship, Australia.

References

1. Lotz B (2000) Eur Phys J 3:185
2. Tjong SC, Li RKY, Cheung T (1997) Polym Eng Sci 37:166
3. Karger-Kocsis J (1996) Polym Eng Sci 36:203
4. Varga J, Schulek-Tóth F, Ille A (1991) Colloid Polym Sci 269:655
5. Yuan Q, Jiang W, An LJ (2004) Colloid Polym Sci 282:1236
6. Hou WM, Liu G, Zhou JJ, Gao X, Li Y, Li Y, Zheng S, Xin Z, Zhao LQ (2006) Colloid Polym Sci 285:11
7. Varga J (2002) J Macromol Sci Part B: Polym Phys 41:1121
8. Padden FJ, Keith HD (1959) J Appl Physiol 30:1479
9. Crissman JM (1969) J Polym Sci 7:389
10. Varga J, Ehrenstein GW (1996) Polymer 37:5959
11. Lovinger AJ, Chua JO, Gryte CC (1977) J Polym Sci Part B: Polym Phys 15:641
12. Schulze GEW, Naujeck TR (1991) Colloid Polym Sci 269:695
13. Pawlak A, Piorkowska E (2001) Colloid Polym Sci 279:939
14. Choi HJ, Cho MS, Kim CA, Jhon MS (1999) Polym Eng Sci 39:1473–1479
15. Grein C (2005) Adv Polym Sci 188:43
16. Karger-Kocsis J (1996) Polym Bull 37:119
17. Karger-Kocsis J (1996) Polym Eng Sci 36:20
18. Varga J, Garzo G (1990) Angew Makromol Chem 180:15
19. Jancar J, Dianselmo A, Dibenedetto AT, Kucera J (1993) Polymer 34:1684
20. Yokoyama Y, Ricco T (1998) Polymer 39:3675
21. Ellul MD, Tsou AH, Hu WG (2004) Polymer 45:3351
22. Wang Y, Zhang Q, Na B, Du RN, Fu Q, Shen KZ (2003) Polymer 44:4261
23. Wang Y, Fu Q, Li QJ, Zhang G, Shen KZ, Wang YZ (2002) J Polym Sci Part B: Polym Phys 40:2086
24. Bai HW, Wang Y, Song B, Li YL, Liu L (2008) J Polym Sci Part B: Polym Phys 46:577
25. Bai HW, Wang Y, Song B, Huang T, Han L (2009) J Polym Sci Part B: Polym Phys 47:46
26. Kim JK, Park JY, Lee KK, Bae CH, Kim SJ (2000) Rubber Technol 1:87
27. Kim JK, Lee SH, Hwang SH (2002) J Appl Polym Sci 85:2276
28. Kim JK, Lee SH (2002) Rubber World 225:26
29. van Duin M (2006) Macromol Symp 233:11
30. Tang XG, Bao RY, Yang W, Xie BH, Yang MB, Meng H (2009) Eur Polym J 45:1448
31. Tang XG, Yang W, Bao RY, Shan GF, Xie BH, Yang MB, Hou M (2009) Polymer 50:4122
32. Turner-Jones A, Aizlewood JM, Beckett DR (1964) Makromol Chem 75:134
33. Yang B, Fu XR, Yang W, Huang L, Yang MB, Feng JM (2008) Polym Eng Sci 48:1707
34. Bai Y, Yin B, Fu XR, Yang MB (2006) J Appl Polym Sci 102:2249
35. Pethrick RA. Polymer structure characterization: from nona to macro organization. p 21
36. Gibbs JW (1906) The scientific work of J. Willard Gibbs, Vol. 1. Longmans Green, New York, p 219
37. Lee KWD, Chan PK, Feng XS (2003) Macromol Theory Simul 12:413
38. Li WB, Zhang KJ, Sengers JV, Gammon RW, Zárate JMOD (1998) Phys Rev Let 81:5580
39. Morse TF, Cipolla JW (1984) J Colloid Int Sci 97:137
40. Subramanian RS (1981) AIChE J 27:646
41. Law BM, Nieuwoudt JC (1989) Phys Rev A40:3880; Velasco RM, García-Colín (1991) J Phys A 24:1007